British Journal of Applied Science & Technology
6(5): 508-519, 2015, Article no.BJAST.2015.106
ISSN: 2231-0843

SCIENCEDOMAIN *international*
www.sciencedomain.org

Biomechanical Analysis for Low Lumbar Spine Segment Fusion with Different Cage Locations

Yugang Jiang[1], Xiongqi Peng[1*], Yu Wang[2*], Cheng Fu[1], Xiaojiang Sun[3] and Kai Zhang[3]

[1]School of Materials Science and Engineering, Shanghai Jiao Tong University, Shanghai, China.
[2]Pediatric Department, Southwest Hospital of the Third Military Medical University, Chongqing, China.
[3]Department of Orthopaedics, Ninth People's Hospital, School of Medicine, Shanghai Jiao Tong University Shanghai, China.

Authors' contributions

This work was carried out in collaboration between all authors. Author YJ designed the study, performed the analysis, wrote the first draft of the manuscript and managed literature searches. Authors XP and YW guided the whole study and revised the manuscript. Authors CF, XS and KZ managed the analyses of the study. All authors read and approved the final manuscript.

Article Information

DOI: 10.9734/BJAST/2015/15576
Editor(s):
(1) Bingyun Li, Department of Orthopaedics, Nanomedicine Laboratory, Robert C. Byrd Health Sciences Center, School of Medicine, West Virginia University, USA.
Reviewers:
(1) Nitin Gupta, Department of Orthopedics, Cygnus Medicare, India.
(2) Anonymous, Turkey.
Complete Peer review History: http://www.sciencedomain.org/review-history.php?iid=768&id=5&aid=7643

Original Research Article

Received 4th December 2014
Accepted 16th December 2014
Published 6th January 2015

ABSTRACT

Aims: This paper aims to investigate the influence of cage location on the biomechanical behavior of lumbar spine with Transforaminal Lumbar Interbody Fusion (TLIF).
Methodology: Firstly, a three-dimensional finite element (FE) model for L4-L5 low lumbar spine segment is established based on computed tomography scan images of a 30-year-old healthy male volunteer. Flexion, extension, lateral bending and torsion motions are simulated and compared with in-vitro cadaveric test data in the literature to validate the lumbar spine FE model. The intact spine model is then modified to TLIF model with one cage insertion under three different implant angles (30°, 45° and 60°).
Results: Numerical results show that after fusion treatment the stress increases dramatically, and mainly distributes on cage and pedicle screw-rod system. Though 45° fusion does not have the lowest von Mises stress at the pedicle screw-rod system and the cage, it is still within an allowable

**Corresponding authors: E-mail: xqpeng@sjtu.edu.cn, 601170159@qq.com*

strength limit. Besides, 45° fusion has the best balanced stability in four basic physiological motions. So if only one cage uses, the 45° posterior location may be more suitable for L4-L5 interbody fusion than 30° and 60° location.

Conclusion: If only one cage uses, the 45° posterior location may be more suitable for L4-L5 interbody fusion than 30° and 60° location.

Keywords: Biomechanics; finite element method; lumbar spine fusion; cage locations.

1. INTRODUCTION

Degeneration of spinal intervertebral disc is a natural procedure [1]. Some may deteriorate to spinal diseases especially in lumbar spine segment. When serious enough, interbody fusion surgery is necessary to recover spine's normal function. A common way is by cage insertion [2]. The clinical efficacy and biomechanical effect of cage insertion are very difficult to evaluate by follow up clinical observation. For example, there is no consensus on whether cage insertion accelerates degeneration process or not at adjacent levels [3-5]. Through experimental study, some researchers [6-9] investigated the influence of cage shape for the purpose of designing proper cage shape. Via finite element analysis, Kim et al. [10,11] found that fusion treatment would greatly increase spinal segment stiffness regardless using one or two cages. However, changing cage shapes or adding more cages mean more surgical time, increased medical cost [12] and surgical risk [13]. Considering these reasons, some surgeons prefer to use one cage only. For this case, cage location will be a key factor affecting post-surgery spine biomechanical behavior. However, there are very limited research works on this aspect [14].

Prediction on range of motion (ROM) and stress distribution in spinal segment after fusion can provide certain reference significance to make effective surgical schedules. So this paper aims to investigate the biomechanical variation with cage location in the case of one cage insertion under different physical motions such as flexion, extension, lateral bending and torsion, and to determine the best one which is beneficial to rapid recovery and preventing further deterioration. Three common locations used in clinical surgical treatment are considered: 30°, 45° and 60° between cage lengthwise midline and sagittal plane of human, as shown in Fig. 1.

An outline of the remainder of this paper is given as follows: In section 2, the finite element model of low lumbar spine segments is developed, and according to clinic study, materials of different parts are taken from the literature. In section 3, the model is validated. In section 4, the influence of different surgical treatments are discussed. Conclusion is provided in section 5.

2. MATERIALS AND METHODS

2.1 Development of Intact Finite Element Model (L4-L5)

Finite element analysis allows to divide complex spine segment into several regions based on its anatomical structure, and then mesh with various types of elements. Assigned with proper materials, its biomechanical characteristics can be properly reflected. In the present study, a surface model (Fig. 2a) for L4-L5 lumbar spine segment is firstly obtain from thin-sliced (2mm) computed tomography (CT) scans of a 30-year-old healthy male volunteer, corresponding solid model is established and then meshed in Hypermesh software (Fig. 2b). Vertebrae, intervertebral discs, endplates and several ligaments are all included in the model. Finally, FE simulation for four basic human spine daily physiological actions of the L4-L5 lumbar spine segment is carried out in ABAQUS/Explicit.

As shown in Fig. 3, the vertebrae are divided into cortical and cancellous bones, which are represented by a layer of hexahedral solid elements and tetrahedral solid elements, respectively. The thickness of cortical bone is assumed to be 1 mm [15,16]. To avoid complex interaction problem, the nodes at the interface between cortical and cancellous bones are all shared. Bones are assumed to be homogeneous and isotropic with different elastic parameters [11,17-19] as listed in Table 1. Contact surfaces with a distance of 0.5 mm are defined to simulate the facet articulation and uncovertebral joints [20]. The intervertebral disc is divided into annulus fibrosus (AF), nucleus pulposus and superior and inferior endplates. All are meshed with 3D solid elements. The superior and inferior endplates have a thickness of 0.5mm [21] sharing common

nodes on the interfaces with their adjacent vertebrae. They are modeled as linear isotropic materials [22]. About 30–50% volume of the cross-section of disc is defined as nucleus pulposus, and the rest is considered as the disc annulus fibrosus [23]. The nucleus pulposus is assumed to be a nearly incompressible material by given a Poisson's ratio of 0.499 and a low Young's modulus of 1 MPa. Material parameters for each part of the intervertebral disc are listed in Table 1.

The ROM of spine is mainly influenced by the intervertebral discs, so to get accurate results, material property for annulus fibrosus under large deformation should be seriously developed. Annulus fibrosus is often characterized by fiber-reinforced material constructed with several layers of annular ground substance embedded with truss elements representing fibers [24-28]. While using one-dimension rebar elements, the interaction between matrix and fibers is ignored, and also increases meshing difficulty. In present study, a continuum mechanics based fiber reinforced hyperelastic model is employed to characterize the anisotropic nonlinear biomechanical behavior of annuls fibrosus based on Peng's theory [29]. The constitutive relationship in [29] is implemented by a user-defined material (VUANISOHYPER subroutine) in ABAQUS/Explicit. The orientation of fibers is ±30° to the horizontal plane [29,30].

Five kinds of ligaments including anterior longitudinal ligament (ALL), posterior longitudinal ligament (PLL), ligamentum flavum (LF), capsular ligament (CL) and interspinous ligament (ISL) are constructed according to anatomical data [31]. They are assumed as linear elastic membranes which yield tensile loads only.

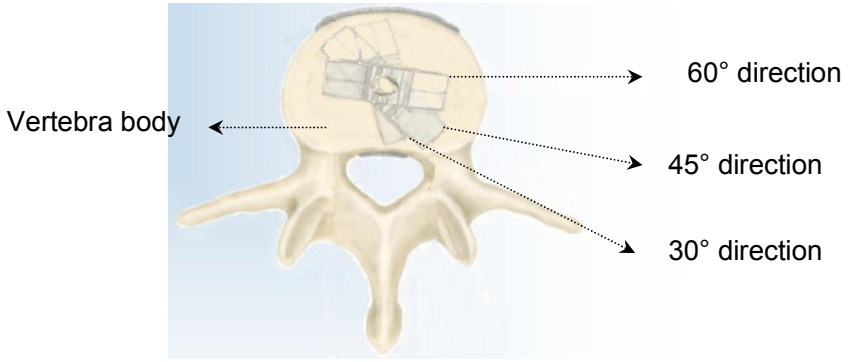

Fig. 1. Scheme map of different cage locations

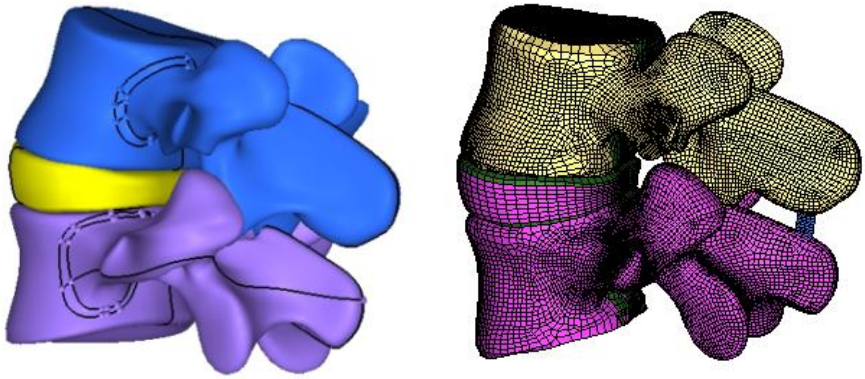

(a) Surface model **(b) FE model**

Fig. 2. The development of FE model

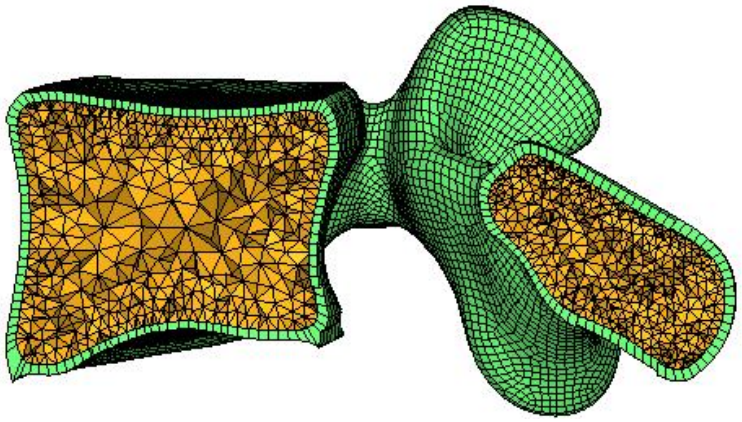

Fig. 3. The sketch map of cortical and cancellous bones (L5)

Table 1. Properties of the materials

Material	Young's modulus E (MPa)	Poisson's ratio v	Reference
Vertebrae			
Cortical bone	12000	0.3	[22,32-37]
Cancellous bone	100	0.2	[22,32,33,36,37]
Endplate	12000	0.3	[34,36,38]
Disc			
Nucleus pulposus	1	0.499	[37,39-41]
Annulus fibrosus	User defined	Material	[29]
Ligaments			
ALL	7.8	0.3	[18,42]
PLL	10	0.3	[18,42]
LF	15	0.3	[18,42]
CL	7.5	0.3	[18,42]
ISL	8	0.3	[18,42]
Cage			
PEEK	3400	0.44	

2.2 DEVELOPMENT OF INTERBODY FUSION FINITE ELEMENT MODEL (L4-L5)

Interbody fusion surgical treatment is to partly recover biomechanical function of degenerated disc by using cage system. Hope to yield and transfer axial force from upper body weight and provide initial three-dimensional stability for lumbar segment. In present study, fusion models are developed from the intact model by a virtual surgery. According to actual surgical treatment, nucleus pulposus is totally removed, while the annulus fibrosus and ligaments are partly persisted by TLIF surgical method. As sketched in Fig. 1, three cage implant locations are considered, which are 30° direction (Model I), 45° direction (Model II) and 60° direction (Model III).

The cage is made by Poly-ether-ether-ketone (PEEK) with dimensions of 36mm×12mm×10mm (length × height × width) (produced by Medtronic Sofamor Danek, Memphis, TN, USA) as shown in Fig. 4a. Notice that some minor features such as location holes and fillets are ignored for the sake of modeling and computational efficiency. Besides, there are many teeth on upper and lower surfaces of the cage to prevent moving during daily physiological motions. Instead of meshing the teeth, a surface to surface contact interaction with a higher friction coefficient of 0.8 is defined between the cage and the adjacent endplates [35].

A posterior pedicle screws-rod system is added to fix the functional spinal unit (FSU). The diameter of rod and screws is 5mm, and the screw length is 45mm. The pedicle and screws

are assumed perfectly bonded without slipping. The "TIE" interaction property is used in ABAQUS to define the interaction between the pedicle screw and vertebral body. In the present model, there is no slipping within the interface between screws and vertebral body. FE models of the pedicle screws-rod system and fusion model are shown in Fig. 5.

2.3 BOUNDARY AND LOADING CONDITIONS

Four basic human spine daily physiological actions including flexion, extension, lateral bending and torsion are simulated. The inferior surface of L5 is completely fixed in all directions. A compressive load 400N and a 10N•m moment are imposed on the superior surface of L4 vertebra along different directions to simulate four physiological motions. Commercially CAE software package ABAQUS/Explicit is used to for the biomechanical FE analysis. Model validations and convergence tests on the FSU are first carried out.

3. RESULTS AND DISCUSSION

3.1 Model Validation and Roms Prediction for Fusion Models

To validate the present model, ROMs of intact L4-L5 FSU under flexion, extension, lateral bending and torsion are predicted and summarized in Table 2. Experimental and numerical results from the literature [41-49] are also shown in Table 2 for comparison. The ROMs from the literature range from 4.48° to 7.13° for flexion, 2.70°-4.88° for extension, 2.08°-5.64° for lateral bending, and 1.50°-3.41° for torsion. For the present model, the ROMs are 4.13°, 3.25°, 3.1° and 3.2° for the four motions, respectively, which are compatible with the reported literature data.

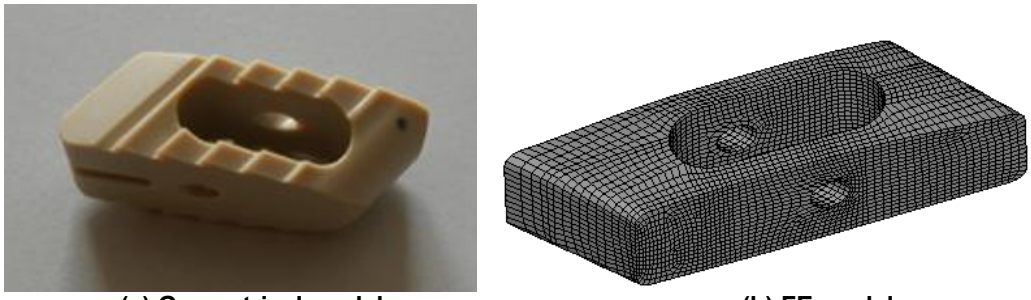

(a) Geometrical model **(b) FE model**

Fig. 4. geometrical model and FE model of the cage

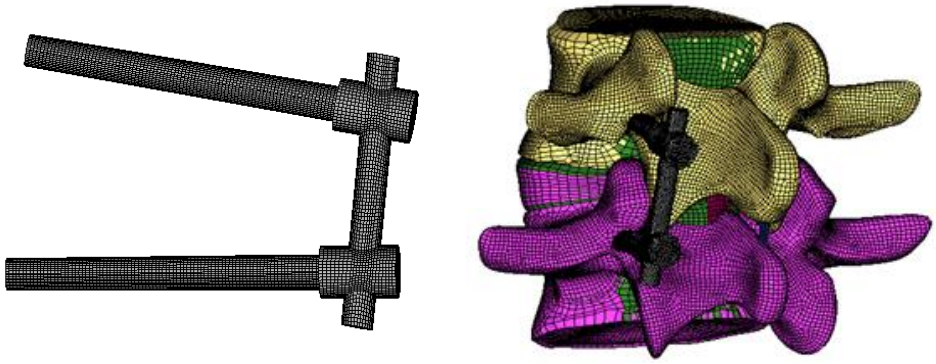

(a) Pedicle screws-rod system **(b) Fusion model**

Fig. 5. Fusion finite element models

Table 2. ROMs in different loading conditions (L4/5 FSU, Unit: degree)

Group	Flexion	Extension	Lateral Bending	Torsion
Goel [45]	FE: 4.828 Exp:5.020±2.824	FE: -3.517 Exp:-4.00±0.980	---	---
Goel [46]	FE: 4.483 Exp:6.183±2.155	FE: -3.345 Exp:-3.241±1.69	FE: 4.517 Exp:4.276±1.655	FE: 2.724 Exp:2.310±0.914
Dooris [44]	FE:5.88	FE: -3.7	---	---
Kiapou [49]	FE: 5.00	FE: -2.70	FE: 4.50	FE: 2.40
Rohlmann [47]	Exp:7.135±2.331	Exp:-4.888±0.955	Exp:3.458±1.354	Exp:3.417±1.354
Chen [48]	FE:5.20	FE:-4.343	FE:4.914	FE:2.829
Chen [42]	FE:4.49	FE:-3.89	FE:2.08	FE:2.08
Grosland [43]	FE: 5.081 Exp:5.51±1.00	FE: -3.351 Exp:-2.99±1.02	FE: 5.181 R.Exp:5.64±1.22 L.Exp:4.90±0.79	FE: 2.75 Exp:1.50±0.67
Present study	FE:4.13	FE:3.25	FE:3.1	FE:3.2

After model validation, the ROMS under the designed various surgical options are compared. With the implantation of the cage (30° fusion) and posterior pedicle screw-rod system, the ROMs decrease about 50%, 60%, 46% and 44% for flexion, extension, lateral bending and torsion, respectively, as shown in Fig. 6. The implant angle has less effect on the ROMs for flexion and torsion. For extension, the ROMs increase from with the increase of implant angle. While a reverse tendency is observed for lateral bending.

3.2.1 Stress in adjacent disc and vertebrae

A typical stress distribution in endplate after intervertebral fusion is shown in Fig. 7 (30° fusion, flexion). Stress concentration mainly appears on the contact region with the cage, and has a maximum stress around 35.3MPa. For 45° and 60° models, the maximum stresses reach 40.4MPa and 31.8 MPa, respectively. The predicted maximum stresses of different anatomical structures under the four physiological motions are listed in Table 3.

As shown in Fig. 8(b), annulus fibrosus are maximum remained when inserting the cage for fusion. The maximum stress under 30° fusion in the remained annulus fibrosus is about 0.49 MPa under flexion, while it is 1.35MPa in the intact model. The maximum stresses in the annulus fibrosis for extension, lateral bending and torsion are also listed in Table 3. It can be found that the maximum stresses decrease more than 60% because of partly excised, but less influenced by cage implant angle.

Fig. 9 shows the stress distribution in the cage. As shown in Fig. 9, the stress concentrates in two regions: (a) the interaction edge between cage and endplate, especially in the region yielding compressive stress; (b) the region around holes. Maximum stress of cage appears in Model III for lateral bending, which reaches nearly 87.5 MPa in all motions, detailed in Table 3. As the cage implant angle increases, the maximum von Mises stress decreases dramatically about 20% for flexion. While for extension, the stress has an obviously increase at 45°, then decreases. For lateral bending and torsion, little variation occurs for three models (Fig. 10).

Fig. 11 shows the Von Mises stress distribution on the external part of the pedicle screws-rod system under different motions. The maximum stress appears at the joint between screw and rod in the case of flexion. As listed in Table 3, the maximum stress under flexion is larger than under extension, lateral bending and torsion, and even reaches nearly 186 MPa in Model III.

For flexion, extension and lateral bending, the maximum stress mainly concentrates on the rod, especially at the surface close to the screw, which yields tensile load. While for torsion, the peak stress appears at the interface between the intervertebral body and screws, it may due to most energy is dissipated by the interaction of these two parts in order to prevent screws' pulling out. The stress values change with cage location are also listed in Table 3. As can be seen from Fig. 12, peak stress dramatically increases about 60% and 54% with the increase of implant angle for flexion and extension, respectively. While for lateral bending, the stress declines about 20%, and there is little variation for torsion, which is around 90 MPa.

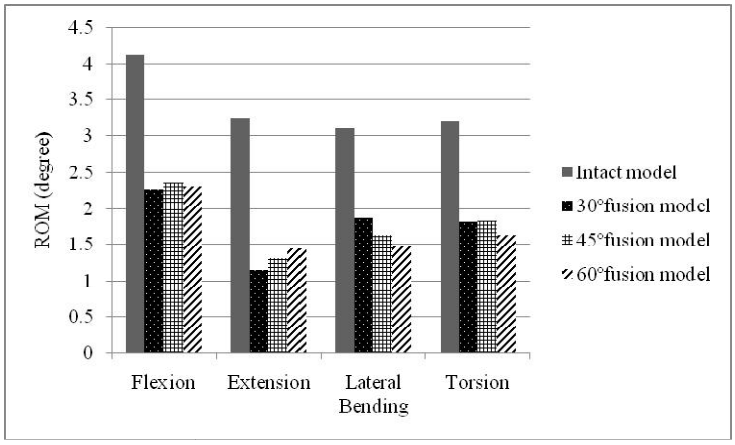

Fig. 6. ROMs for different fusion models

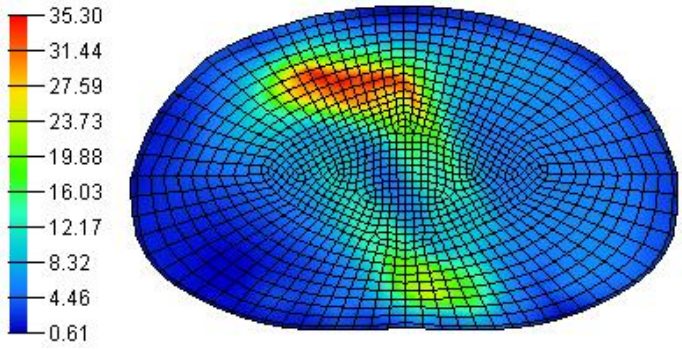

Fig. 7. Typical Von Mises stress distribution of endplate (30° fusion, flexion)

Table 3. Maximum stress in different structures (Unit: MPa)

		Flexion	Extension	Lateral bending	Torsion
Model I	Endplate	35.3	31.0	38.3	36.7
	AF	0.48	0.18	0.96	0.51
	L4 cortical	57.3	35.3	32.7	55.9
	L5 cortical	49.1	29.9	44.4	44.9
	cage	67.2	47.4	57.7	82.8
	screws-rod system	116.1	104.5	119.5	95.0
Model II	Endplate	40.4	31.3	40.2	30.1
	AF	0.59	0.19	0.54	0.79
	L4 cortical	49.4	37	32.6	57.6
	L5 cortical	51.0	31.1	39.2	47.7
	cage	65.4	56.1	86.3	71.5
	screws-rod system	143.1	143.5	92.8	92.1
Model III	Endplate	31.8	27.5	38.5	35.9
	AF	0.42	0.13	0.38	0.35
	L4 cortical	56.7	33.2	42.4	52.1
	L5 cortical	50.1	30.9	50.2	41.9
	cage	54.0	48.6	87.5	71.1
	screws-rod system	186.8	161.1	95.8	91.4

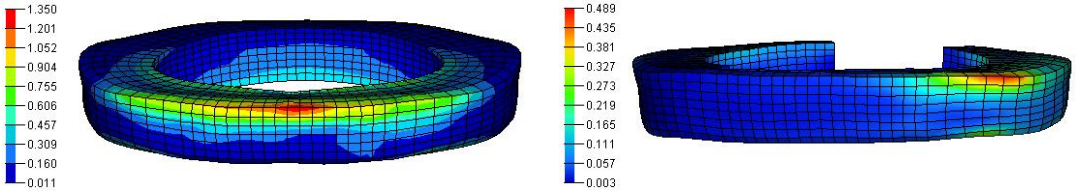

(a) Intact model (b) 30° fusion, flexion

Fig. 8. Von Mises stress contributions in annulus fibrosus

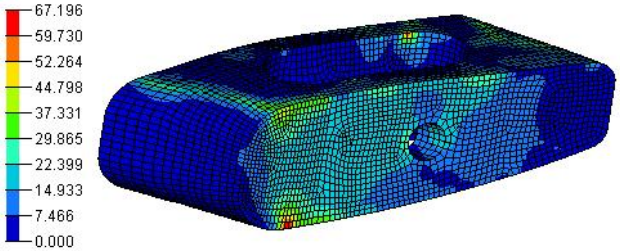

Fig. 9. Stress distribution in cage (30° fusion, flexion)

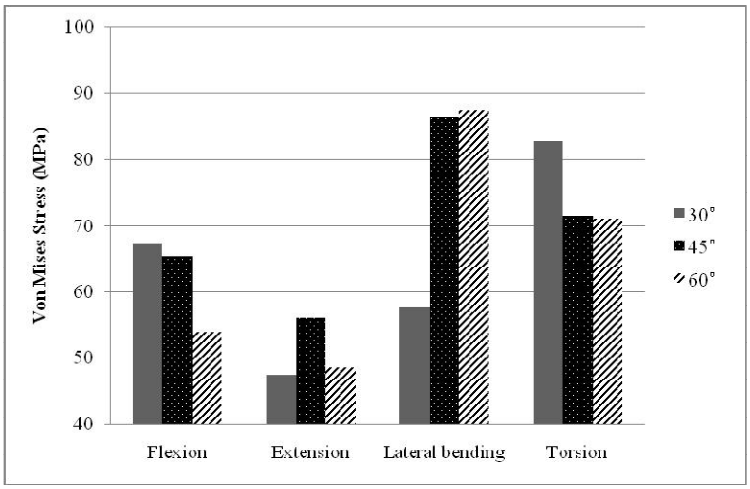

Fig. 10. Von Mises Stress distribution in cage (30° fusion, flexion)

The numerical results of fusion model indicate that the cage location changes the biomechanical response of L4/5 FSU. The cage transfers axial force from upper body to lower part instead of nucleus, which weakens the deformation ability, and leads to a decrease of ROMs directly. Synthesizing Table 3 and Figs. 10,12, though Model II (45° fusion) does not have the lowest von Mises stress at pedicle screws-rod system and the cage, it has the best balanced stability in four basic physiological motions both for sagittal and coronal plane. So if only one cage is used, 45° posterior location may be more suitable for L4-L5 interbody fusion than other cage locations.

Present study has some limitations. First, the bones and ligaments are assumed as homogeneous and isotropic materials, while this may be inappropriate in some complex loading conditions or large deformation status. Secondly, the adjacent level degeneration is ignored. Lastly, the interaction between screws and vertebral body is not considered. Our future work will concentrate on developing a more accurate model to comprehend the biomechanical essentials of human spine segment.

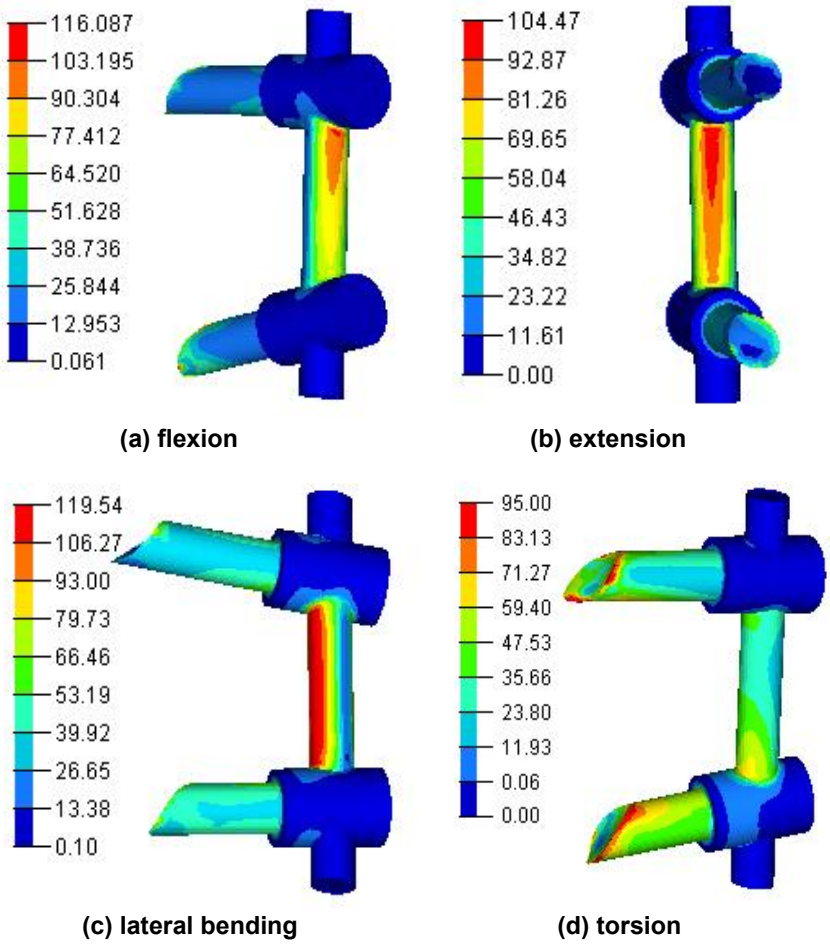

(a) flexion **(b) extension**

(c) lateral bending **(d) torsion**

Fig. 11. von Mises stress distribution in pedicle screws-rod system (30° fusion)

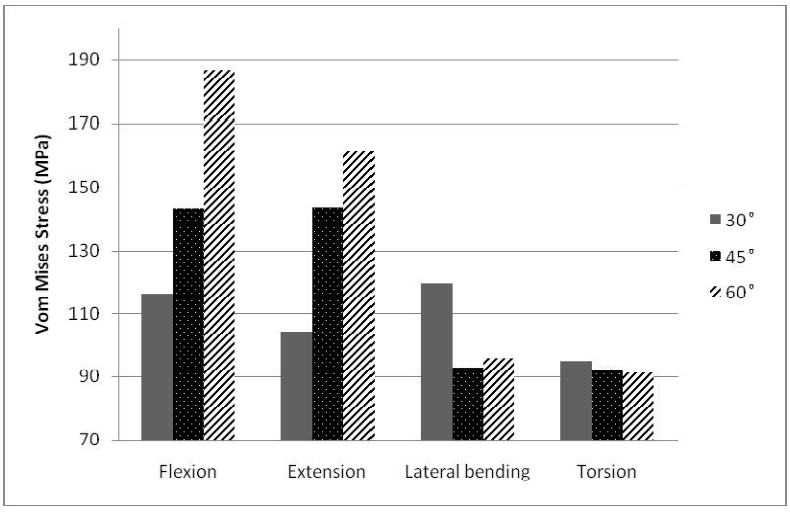

Fig. 12. von Mises stress distribution in pedicle screws-rod system

4. CONCLUSION

In present study a three-dimensional finite element model of L4-L5 fusion spine is established to investigate the effect of cage location on its biomechanical behavior under various daily actions including flexion, extension, lateral bending and torsion motions. The numerical predictions indicate that after fusion, the ROMs reduce about 44%-50% for all four motions. When the cage implant angle increases, the ROMs increase for flexion and extension and decrease for lateral bending, but less fluctuation for torsion. For von Mises stress, as the cage implant angle increases, the maximum stress of cage decreases dramatically about 20% for flexion, and has an obviously increase at 45° then falls at 60° fusion for extension, but little variation occurs for three models for lateral bending and torsion. As for pedicle screws-rod system, the stress mainly concentrates on the rod, especially at the surface close to the screw except torsion, which appears at the interface between the intervertebral body and screws. When cage implant angle increases, the peak stress dramatically increases about 60% and 54% for flexion and extension, while for lateral bending, the stress declines about 20%, and has little variation for torsion. According to present study, though 45° cage location does not have the lowest von Mises stress at pedicle screws-rod system and the cage, it has the best balanced stability in four basic physiological motions. So if only one cage is used, 45° posterior location may be more suitable for L4-L5 interbody fusion than 30° and 60° cage implant location.

ACKNOWLEDGEMENT

The supports from the National Natural Science Foundation of China (11172171), Key Scientific and Technological Project Foundation of Chongqing, China (CSTC2012gg-yyjs10011) are gratefully acknowledged.

COMPETING INTERESTS

Authors have declared that no competing interests exist.

REFERENCES

1. Vernon Roberts B. Disc pathology and disease states. The Biology of the Intervertebral Disc. 1988;2:73-119.
2. McAfee PC. Current concepts review-interbody fusion cages in reconstructive operations on the spine. The Journal of Bone & Joint Surgery. 1999;81:859-880.
3. Rahm MD, Hall BB. Adjacent-segment degeneration after lumbar fusion with instrumentation: A retrospective study. Journal of Spinal Disorders & Techniques. 1996;9:392-400.
4. Seitsalo S, Schlenzka D, Poussa M, Österman K. Disc degeneration in young patients with isthmic spondylolisthesis treated operatively or conservatively: A long-term follow-up. European Spine Journal. 1997;6:393-397.
5. van Ooij A, Oner FC, Verbout AJ. Complications of artificial disc replacement: A report of 27 patients with the SB Charite disc. Spine. 2003;28:369-383.
6. Oxland TR, Lund T. Biomechanics of stand-alone cages and cages in combination with posterior fixation: A literature review. European Spine Journal. 2000;9:095-101.
7. Glazer PA, Colliou O, Klisch SM, Bradford DS, Bueff UH, Lotz JC. Biomechanical analysis of multilevel fixation methods in the lumbar spine. Spine. 1997;22:171-182.
8. Tencer AF, Hampton D, Eddy S. Biomechanical properties of threaded inserts for lumbar interbody spinal fusion. Spine. 1995;20:2408-2414.
9. Rapoff AJ, Ghanayem AJ, Zdeblick TA. Biomechanical comparison of posterior lumbar interbody fusion cages. Spine. 1997;22:2375-2379.
10. Kim Y. Prediction of mechanical behaviors at interfaces between bone and two interbody cages of lumbar spine segments. Spine. 2001;26:1437-1442.
11. Kim Y, Vanderby R. Finite element analysis of interbody cages in a human lumbar spine. Computer Methods in Biomechanics and Biomedical Engineering. 2000;3:257-272.
12. Molinari RW, Sloboda J, Johnstone FL. Are 2 cages needed with instrumented PLIF? A comparison of 1 versus 2 interbody cages in a military population. American Journal of Orthopedics (Belle Mead, NJ). 2003;32:337.
13. Okuyama K, Abe E, Suzuki T, Tamura Y, Chiba M, Sato K. Posterior lumbar interbody fusion: A retrospective study of complications after facet joint excision and

pedicle screw fixation in 148 cases. Acta Orthopaedica. 1999;70:329-334.
14. Cheng K, Chen S, Liu CL. Biomechanical analysis of the lumbar spine with anterior interbody fusion on the different locations of the bone grafts. Bio-medical materials and engineering. 2002;12:367-374.
15. Goel VK, Kim YE, Lim T, Weinstein JN. An analytical investigation of the mechanics of spinal instrumentation. Spine. 1988;13:1003-1011.
16. Lu YM, Hutton WC, Gharpuray VM. Do bending, twisting, and diurnal fluid changes in the disc affect the propensity to prolapse? A viscoelastic finite element model. Spine. 1996;21:2570-2579.
17. Goel VK, Ramirez SA, Kong W, Gilbertson LG. Cancellous bone Young's modulus variation within the vertebral body of a ligamentous lumbar spine-application of bone adaptive remodeling concepts. Journal of Biomechanical Engineering. 1995;117:266-271.
18. Pitzen T, Geisler F, Matthis D, Müller Storz H, Barbier D, Steudel WI, Feldges A. A finite element model for predicting the biomechanical behaviour of the human lumbar spine. Control Engineering Practice. 2002;10:83-90.
19. Lee KK, Teo EC, Fuss FK, Vanneuville V, Qiu TX, Ng HW, Yang K, Sabitzer RJ. Finite-element analysis for lumbar interbody fusion under axial loading. Biomedical Engineering, IEEE Transactions on. 2004;51:393-400.
20. Zander T, Rohlmann A, Calisse J, Bergmann G. Estimation of muscle forces in the lumbar spine during upper-body inclination. Clinical Biomechanics. 2001;16:73-80.
21. Silva M, Wang C, Keaveny T, Hayes W. Direct and computed tomography thickness measurements of the human, lumbar vertebral shell and endplate. Bone. 1994;15:409-414.
22. Goel VK, Ramirez SA, Kong W, Gilbertson LG. Cancellous bone Young's modulus variation within the vertebral body of a ligamentous lumbar spine—application of bone adaptive remodeling concepts. Journal of Biomechanical Engineering. 1995;117:266-271.
23. Panagiotacopulos ND, Pope MH, Krag MH, Block R. Water Content in Human Intervertebral Discs: Part I. Measurement by Magnetic Resonance Imaging. Spine. 1987;12:912-917.
24. Sairyo K, Goel VK, Vadapalli S, Vishnubhotla SL, Biyani A, Ebraheim N, Terai T, Sakai T. Biomechanical comparison of lumbar spine with or without spina bifida occulta. A finite element analysis. Spinal Cord. 2006;44:440-444.
25. Chen SH, Tai CL, Lin CY, Hsieh PH, Chen WP. Biomechanical comparison of a new stand-alone anterior lumbar interbody fusion cage with established fixation techniques - a three-dimensional finite element analysis. BMC Musculoskeletal Disorders. 2008;9:88.
26. Kuo CS, Hu HT, Lin RM, Huang KY, Lin PC, Zhong ZC, Hseih ML. Biomechanical analysis of the lumbar spine on facet joint force and intradiscal pressure-a finite element study. BMC Musculoskeletal Disorders. 2010;11:151.
27. Kim KT, Lee SH, Suk KS, Lee JH, Jeong BO. Biomechanical changes of the lumbar segment after total disc replacement: Charite®, Prodisc® and Maverick® using finite element model study. Journal of Korean Neurosurgical Society. 2010;47:446-453.
28. Chen SH, Zhong ZC, Chen CS, Chen WJ, Hung C. Biomechanical comparison between lumbar disc arthroplasty and fusion. Medical Engineering & Physics. 2009;31:244-253.
29. Peng X, Guo Z, Moran B. An anisotropic hyperelastic constitutive model with fiber-matrix shear interaction for the human annulus fibrosus. Journal of Applied Mechanics. 2006;73:815-824.
30. Ruberté LM, Natarajan RN, Andersson GB. Influence of single-level lumbar degenerative disc disease on the behavior of the adjacent segments—a finite element model study. Journal of Biomechanics. 2009;42:341-348.
31. Agur A, Lee M. Grant's Atlas of anatomy 10th ed. In. Philadelphia: Lippincott Williams & Wilkins; 1999.
32. Panjabi M, Oxland T, Yamamoto I, Crisco J. Mechanical behavior of the human lumbar and lumbosacral spine as shown by three-dimensional load-displacement curves. Journal of Bone and Joint Surgery-A-American Volumes. 1994;76:413-424.
33. Natarajan R, Andersson G. Modeling the annular incision in a herniated lumbar intervertebral disk to study its effect on disk stability. Computers & structures. 1997;64:1291-1297.

34. Pitzen T, Geisler FH, Matthis D, Müller Storz H, Pedersen K, Steudel WI. The influence of cancellous bone density on load sharing in human lumbar spine: A comparison between an intact and a surgically altered motion segment. European Spine Journal. 2001;10:23-29.
35. Polikeit A, Ferguson SJ, Nolte LP, Orr TE. Factors influencing stresses in the lumbar spine after the insertion of intervertebral cages: Finite element analysis. European Spine Journal. 2003;12:413-420.
36. Denoziere G. Numerical modeling of a ligamentous lumbar motion segment. 2004.
37. Sairyo K, Goel VK, Masuda A, Vishnubhotla S, Faizan A, Biyani A, Ebraheim N, Yonekura D, Murakami RI, Terai T. Three-dimensional finite element analysis of the pediatric lumbar spine. Part I: Pathomechanism of apophyseal bony ring fracture. European Spine Journal. 2006;15:923-929.
38. Wilke HJ, Neef P, Caimi M, Hoogland T, Claes LE. New *In vivo* measurements of pressures in the intervertebral disc in daily life. Spine. 1999;24:755-762.
39. Smit TH, Odgaard A, Schneider E. Structure and function of vertebral trabecular bone. Spine. 1997;22:2823-2833.
40. Ng HW, Teo EC. Nonlinear finite-element analysis of the lower cervical spine (C4–C6) under axial loading. Journal of Spinal Disorders & Techniques. 2001;14:201-210.
41. Rohlmann A, Zander T, Schmidt H, Wilke H-J, Bergmann G. Analysis of the influence of disc degeneration on the mechanical behaviour of a lumbar motion segment using the finite element method. Journal of Biomechanics. 2006;39:2484-2490.
42. Chen CS, Cheng CK, Liu CL, Lo WH. Stress analysis of the disc adjacent to interbody fusion in lumbar spine. Medical engineering & physics. 2001;23:485-493.
43. Grosland NM. Spinal adaptations in response to interbody fusion systems: A theoretical investigation. University of Iowa; 1998.
44. Dooris AP, Goel VK, Grosland NM, Gilbertson LG, Wilder DG. Load-sharing between anterior and posterior elements in a lumbar motion segment implanted with an artificial disc. Spine. 2001;26:122-129.
45. Goel VK, Grauer JN, Patel TC, Biyani A, Sairyo K, Vishnubhotla S, Matyas A, Cowgill I, Shaw M, Long R. Effects of charite artificial disc on the implanted and adjacent spinal segments mechanics using a hybrid testing protocol. Spine. 2005;30:2755-2764.
46. Goel VK, Mehta A, Jangra J, Faizan A, Kiapour A, Hoy RW, Fauth AR. Anatomic facet replacement system (AFRS) restoration of lumbar segment mechanics to intact: A finite element study and in vitro cadaver investigation. SAS Journal. 2007;1:46-54.
47. Rohlmann A, Burra NK, Zander T, Bergmann G. Comparison of the effects of bilateral posterior dynamic and rigid fixation devices on the loads in the lumbar spine: a finite element analysis. European Spine Journal. 2007;16:1223-1231.
48. Chen SH, Zhong ZC, Chen CS, Chen WJ, Hung C. Biomechanical comparison between lumbar disc arthroplasty and fusion. Medical Engineering & Physics. 2009;31:244-253.
49. Kiapour A, Ambati D, Hoy RW, Goel VK. Effect of graded facetectomy on biomechanics of Dynesys dynamic stabilization system. Spine. 2012;37:581-589.

Peer-review history:
The peer review history for this paper can be accessed here:
http://www.sciencedomain.org/review-history.php?iid=768&id=5&aid=7643